Mapping bias-induced phase stability and random fields in relaxor ferroelectrics

B. J. Rodriguez,[1,a)] S. Jesse,[2] A. A. Bokov,[3] Z.-G. Ye,[3] and S. V. Kalinin[2,b)]
[1]*University College Dublin, Belfield, Dublin 4, Ireland*
[2]*Oak Ridge National Laboratory, Oak Ridge, Tennessee 37831, USA*
[3]*Department of Chemistry and 4D LABS, Simon Fraser University, Burnaby, British Columbia V5A 1A6, Canada*

(Received 15 May 2009; accepted 15 August 2009; published online 4 September 2009)

The spatial variability of polarization reversal behavior in the relaxor $0.9Pb(Mg_{1/3}Nb_{2/3}O_3)-0.1PbTiO_3$ crystal, is revealed on the ~100 nm scale using switching spectroscopy piezoresponse force microscopy. Quenched fields conjugate to polarization are found, which show mesoscopic (~100–200 nm) spatial fluctuations around near-zero bias values. The mapping of the stability gap of the bias-induced phase and conjugate random fields is demonstrated. The origin of the observed nanoscale domains and the field-induced part of the polarization are discussed. © *2009 American Institute of Physics*. [DOI: 10.1063/1.3222868]

Ferroelectric relaxors have attracted much attention as prospective materials for acoustic and medical imaging applications.[1] The unique properties of relaxors are traditionally associated with the presence of polar nanoregions (PNRs), the formation and transformations of which result in a broad spectrum of dynamic temperature- and field-induced behaviors. Despite recent progress in understanding relaxor behavior,[2,3] a number of aspects remain unresolved, including the polarization switching mechanisms (rotation versus wall motion) and observations of Barkhausen noise during polarization reversal, among others.[4] The development of piezoresponse force microscopy (PFM) in the past decade has precipitated several studies of mesoscopic domain polarization distributions in relaxor ferroelectrics, including observations of fractal domain walls in the nonergodic phase of relaxors,[5–7] ferroelectric domains in uniaxial relaxors,[8,9] and persistent labyrinthine domains of spontaneous polarization in the macroscopically nonpolar "ergodic" relaxor phase.[6,10,11] Complementary to imaging static domain patterns, piezoresponse force spectroscopy[12] was used to study local polarization dynamics in relaxors.[6] These experiments are analogous to macroscopic bias-induced experiments, allowing the phase-field diagram of relaxor ferroelectrics to be sampled locally.

Observations of complex *static* mesoscopic polarization patterns in relaxor materials suggest the corresponding dynamic behavior and bias-induced phase transitions can also be position dependent. Quenched electric random fields are believed to be responsible[10] for the alignment of PNRs which lead to the appearance of polar domains, as suggested by the earlier work of Imry and Ma[13] on magnetic systems. Westphal *et al.*[14] further showed that the stability of the domain state is tied to the local fluctuations of the random fields. Recently, Shvartsman *et al.*[15] suggested that these polar domains are the quasistatic PNRs themselves (precursors of ferroelectric domains), which are frozen due to their comparatively large size, and that small dynamic PNRs are located between them. The polar, labyrinthine domain shape, roughness, and size are likely dictated by the interplay between strain accommodation as discussed in detail in Ref. 15 and ordering forces including but not limited to the quenched electric random fields. A different model suggested[16] that each polar domain consists of a large number of static and dynamic PNRs embedded into a nonpolar matrix. The dipole moments of the static PNRs are fixed in orientation, while the dynamic PNRs are unstable against thermal agitation. Recently, an approach for nanoscale mapping of random-field and random-bond disorder potential components has been demonstrated for normal ferroelectrics.[17] Here, we study the spatial uniformity of polarization reversal at the surface of a relaxor crystal using switching spectroscopy PFM (SS-PFM).[18]

The $(1-x)Pb(Mg_{1/3}Nb_{2/3})O_3-x$ $PbTiO_3$ crystal with $x=0.1$ (PMN-10%PT) is grown from high temperature solution and has a dielectric maximum at $T_{max}=310$ K (at 1 kHz).[19] The crystal undergoes a phase transition to a rhombohedral ferroelectric state on cooling at $T_c \cong 280$ K,[20] thus the measurements are performed in the macroscopically cubic "ergodic" relaxor state (note that a surface phase can exist in the frozen state due to, e.g., strain effects).[21] The PFM and SS-PFM measurements are performed on the mirror-polished (001) crystal surface using a commercial atomic force microscope system (Veeco MultiMode NS-IIIA), which was modified as described elsewhere.[18] During SS-PFM, hysteresis loops are measured at every point in a mesh grid (a 40×40 array with a 12.5 nm step size) and analyzed to yield two-dimensional maps of switching properties including imprint, switching bias, and the area within the loop (i.e., the work of switching). In SS-PFM, the writing and reading state durations were 39.06 ms, while the 15 ms measurement window immediately followed a 15 ms delay from the end of the writing state. PFM and SS-PFM data were acquired with a 615 kHz, 2 V bias to the tip (Mikromasch Au-Cr coated Si tip, with spring constant $k \sim 0.6$ N/m).

The surface topography and the corresponding domain structure (PFM phase) images are shown in Figs. 1(a) and 1(b). The PFM phase image demonstrates the labyrinthine structure typical of relaxors in the "ergodic" bulk phase.

a)Electronic mail: brian.rodriguez@ucd.ie.
b)Author to whom correspondence should be addressed. Electronic mail: sergei2@ornl.gov.

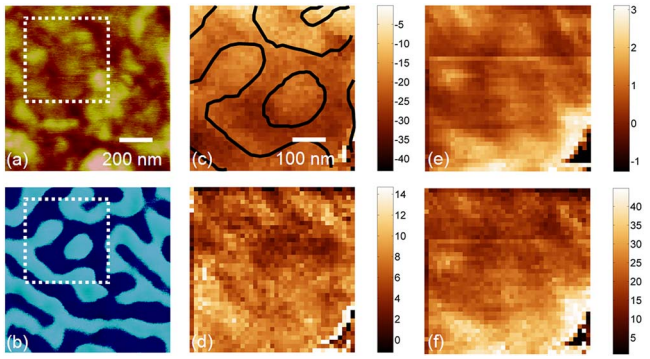

FIG. 1. (Color online) (a) Surface topography (5 nm *z*-scale) and (b) PFM phase signal of the PMN-10PT crystal surface. (c) Positive and (d) negative coercive bias SS-PFM maps. (e) Map of switchable polarization. (f) Work of switching SS-PFM map. The pixel size in panels [(c)–(f)] is 12.5 nm. The black lines in (c) are a contour map overlay of (b).

Dark and bright areas in this image correspond to polar domains of static polarization directed upwards and downwards, respectively.

To explore the polarization dynamics on relaxor surfaces, we performed SS-PFM mapping within the same region. The hysteresis loops from selected locations are shown in Fig. 2. They are shifted to negative bias values and loops from adjacent locations show close similarity, suggesting the measurements are performed in the dense regime [note that the pixel size is smaller than the tip radius (nominally 50 nm)]. At the same time, significant variability between well-separated points (~100–200 nm) is observed. Positive and negative coercive bias SS-PFM maps are shown in Figs. 1(c) and 1(d), while SS-PFM maps of the reversible polarization and the work of switching are shown in Figs. 1(e) and 1(f). Note the lack of one to one correspondence between topography, PFM, and SS-PFM maps (within the limitations imposed by the thermal drift of the microscope), illustrating the complementary nature of the data.

The hysteresis loop shape in PFM describes the convolution between the bias-induced change in material properties and the signal generation volume in a PFM experiment. In classical ferroelectrics, the material evolution can be well described as the sequential intrinsic domain nucleation and subsequent domain growth by wall motion.[22] A number of observations suggest that the polarization reorientation mechanism in relaxors is drastically different, and proceeds through a gradual evolution and decay of bias-induced states[16,23] similarly to the macroscopic case.[24] Comparison with relaxation studies suggests that the loops in PMN-10%PT are related to a large bias-induced polarization with a relaxation time of ~10 s,[16] i.e., much longer than the dc bias cycling in the SS-PFM experiments.

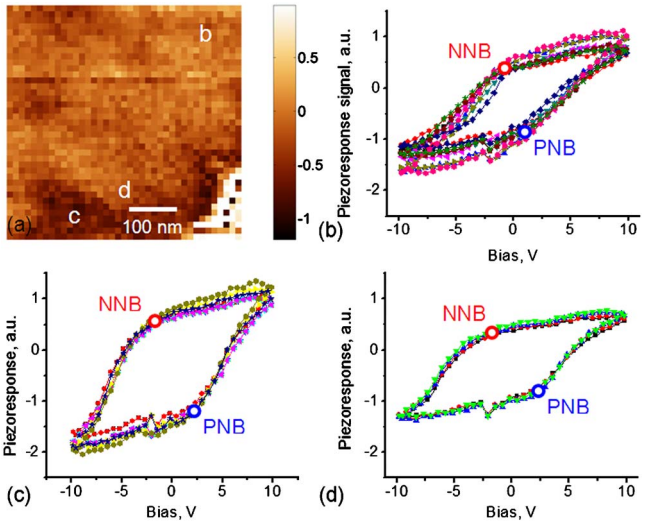

FIG. 2. (Color online) (a) Piezoresponse SS-PFM map and [(b)–(d)] hysteresis loops from selected locations. The lower right corner in (a) is a region exhibiting an experimental artifact. PNB and NNB are indicated in [(b)–(d)]. Note that the PNB and NNB in (b) are close to zero. Panel a has a 12.5 nm pixel size and was acquired simultaneously with Figs. 1(c)–1(f).

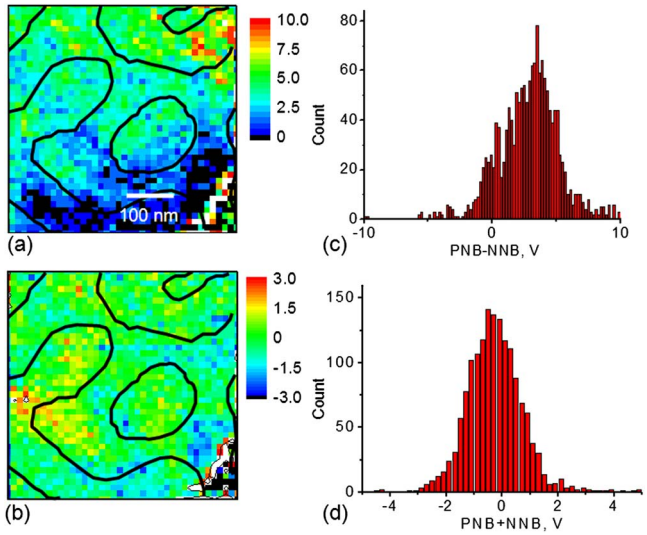

FIG. 3. (Color online) (a) Stability gap and (b) built-in field maps and [(c) and (d)] corresponding histograms. Panels (a) and (b) were constructed from the same SS-PFM data set shown partially in Figs. 1 and 2 and have a 12.5 nm pixel size. The black lines in (a) and (b) represent domain walls.

Note that some hysteresis loops have nearly overlapping or in some cases, overlapping values of positive and negative nucleation biases (PNB and NNB, respectively) suggesting that the bias-induced state is unstable. We propose that the value of the stability gap (SG), SG=(PNB−NNB) provides a measure of the absolute stability of the bias-induced phase, with SG>0 corresponding to thermodynamically or kinetically stable bias-induced state, and SG<0 corresponding to an unstable state. Furthermore, independent of the microscopic origin of the loops in PMN-10%PT, the influence of the built-in field is expected to be similar, namely, the loop is shifted in a horizontal direction (the effect known as imprint in ferroelectric materials). Hence, PNB+NNB allows mapping of built-in fields as proposed earlier.[17]

The stability gap and built-in field maps for a PMN-10%PT crystal surface are shown in Figs. 3(a) and 3(b). The two maps are generally uncorrelated, indicative of the veracity of the measurements. The corresponding histograms of PNB−NNB and PNB+NNB are shown in Fig. 3(c) and 3(d). The images show large scale features, characteristic of the presence of disorder in the material on the mesoscopic scale. In the built-in field map [Fig. 3(b)], regions of positive (yellow and red) and negative (blue) fields separated by the regions (green) where the field is close to zero can be observed. This picture corresponds to the frozen fluctuations of the local field with a period of ~100–200 nm and differs drastically from that found in the normal ferroelectric phase of lead zirconate titanate (PZT).[17] In PZT, a rather abrupt

alternation of the field sign can be observed and a number of pointlike defects associated with a single pixel are found. The field distribution [Fig. 3(d)] is centered near zero, which means that on the macroscopic scale, the near-surface field is absent or much smaller than the amplitude of the local field fluctuations.

In the framework of the picture of static and dynamic PNRs (Ref. 16) our current results suggest that the polarization of static PNRs (labyrinthine domains) are not switched by external electric field and that their configuration after the application of dc bias remains unchanged. The observed comparatively large bias-induced polarization can be due to the reorientation of the dynamic PNRs, variation of the size of the dynamic PNRs, and, in stronger fields, due to the transition into a metastable ferroelectric phase. Though the spatial inhomogeneities of characteristics of bias-induced polarization, including stability gap [Fig. 3(a)], switchable polarization [Fig. 1(e)], and work of switching [Fig. 1(f)] are correlated, they reveal no direct correlation with the labyrinthine domain structure [Fig. 1(b)], which confirms a different origin and the relative independence of the labyrinthine domains (created by static PNRs) and the bias-induced polarization (coming from reorientations of dynamic PNRs, and, possibly, the growth of their size).

To summarize, the spatial variability of polarization switching on a PMN-10%PT crystal relaxor ferroelectric surface is studied by SS-PFM. The SS-PFM maps reveal a significant variability of switching behavior associated with mesoscopic disorder. The static labyrinthine domain pattern does not correlate directly with the distribution of quenched local fields at the surface of the relaxor crystal, indicating that the fields are not the sole cause of the domain formation. The mapping of the stability gap for the bias-induced phase and the built-in field distributions is demonstrated, illustrating the presence of quenched random fields with mesoscopic ($\sim$100–200 nm) inhomogeneities.

This research is supported (B.J.R., S.J., and S.V.K.) by the Division of Scientific User Facilities, Office of Basic Energy Sciences, U.S. Department of Energy and was part of a CNMS User Program (Grant No. CNMS2007-085). The work is also supported (A.A.B. and Z.G.Y.) by the Office of Naval Research (Grant No. N00014–06–1–0166). B.J.R. also acknowledges the support of UCD Research.

[1] Y. Yamashita, Springer Ser. Mater. Sci. **114**, 223 (2008).
[2] L. E. Cross, Ferroelectrics **76**, 241 (1987).
[3] A. A. Bokov and Z. G. Ye, J. Mater. Sci. **41**, 31 (2006).
[4] E. V. Colla, L. K. Chao, and M. B. Weissman, Phys. Rev. Lett. **88**, 017601 (2001).
[5] F. Bai, J. Li, and D. Viehland, J. Appl. Phys. **97**, 054103 (2005).
[6] V. V. Shvartsman, A. L. Kholkin, A. Orlova, D. Kiselev, A. A. Bogomolov, and A. Sternberg, Appl. Phys. Lett. **86**, 202907 (2005).
[7] V. V. Shvartsman, W. Kleemann, T. Łukasiewicz, and J. Dec, Phys. Rev. B **77**, 054105 (2008).
[8] P. Lehnen, W. Kleemann, T. Woike, and R. Pankrath, Phys. Rev. B **64**, 224109 (2001).
[9] W. Kleemann, G. A. Samara, and J. Dec, in *Polar Oxides: Properties, Characterization, and Imaging*, edited by R. Waser, U. Böttger, and S. Tiedke (Wiley, Weinheim, 2005).
[10] W. Kleemann, J. Dec, V. V. Shvartsman, Z. Kutnjak, and T. Braun, Phys. Rev. Lett. **97**, 065702 (2006).
[11] V. V. Shvartsman and A. L. Kholkin, J. Appl. Phys. **101**, 064108 (2007).
[12] A. N. Morozovska, E. A. Eliseev, S. Jesse, B. J. Rodriguez, and S. V. Kalinin, J. Appl. Phys. **102**, 114108 (2007).
[13] Y. Imry and S.-K. Ma, Phys. Rev. Lett. **35**, 1399 (1975).
[14] V. Westphal, W. Kleemann, and M. D. Glinchuk, Phys. Rev. Lett. **68**, 847 (1992).
[15] V. V. Shvartsman, J. Dec, T. Lukasiewicz, A. L. Kholkin, and W. Kleemann, Ferroelectrics **373**, 77 (2008).
[16] S. V. Kalinin, B. J. Rodriguez, J. D. Budai, S. Jesse, A. N. Morozovska, A. A. Bokov, and Z.-G. Ye, e-print arXiv:0808.3827v1.
[17] S. Jesse, B. J. Rodriguez, S. Choudhury, A. P. Baddorf, I. Vrejoiu, D. Hesse, M. Alexe, E. A. Eliseev, A. N. Morozovska, J. Zhang, L. Q. Chen, and S. V. Kalinin, Nature Mater. **7**, 209 (2008).
[18] S. Jesse, H. N. Lee, and S. V. Kalinin, Rev. Sci. Instrum. **77**, 073702 (2006).
[19] M. Dong and Z. G. Ye, J. Cryst. Growth **209**, 81 (2000).
[20] Z. G. Ye, Y. Bing, J. Gao, A. A. Bokov, P. Stephens, B. Noheda, and G. Shirane, Phys. Rev. B **67**, 104104 (2003).
[21] V. V. Shvartsman, J. Dec, T. Łukasiewicz, A. L. Kholkin, and W. Kleemann, Ferroelectrics **373**, 77 (2008).
[22] S. Jesse, A. P. Baddorf, and S. V. Kalinin, Appl. Phys. Lett. **88**, 062908 (2006).
[23] V. V. Shvartsman, A. L. Kholkin, M. Tyunina, and J. Levoska, Appl. Phys. Lett. **86**, 222907 (2005).
[24] B. Dkhil, J. M. Kiat, G. Calvarin, G. Baldinozzi, S. B. Vakhrushev, and E. Suard, Phys. Rev. B **65**, 024104 (2001).